Journal of Molecular Structure 1233 (2021) 130112

Contents lists available at ScienceDirect

Journal of Molecular Structure

journal homepage: www.elsevier.com/locate/molstr

Synthesis, spectral characterization, crystal structure and antibacterial activity of nickel(II), copper(II) and zinc(II) complexes containing ONNO donor Schiff base ligands

Hadi Kargar[a,*], Amir Adabi Ardakani[b], Muhammad Nawaz Tahir[c], Muhammad Ashfaq[c], Khurram Shahzad Munawar[d,e]

[a] Department of Chemical Engineering, Faculty of Engineering, Ardakan University, P.O. Box 184, Ardakan, Iran
[b] Department of chemistry, Ardakan Branch, Islamic Azad University, Ardakan, Iran
[c] Department of Physics, University of Sargodha, Punjab, Pakistan
[d] Department of Chemistry, University of Sargodha, Punjab, Pakistan
[e] Department of Chemistry, University of Mianwali, Mianwali, Pakistan

ARTICLE INFO

Article history:
Received 17 January 2021
Revised 7 February 2021
Accepted 8 February 2021
Available online 16 February 2021

Keywords:
Schiff base complex
Spectral characterization
X-ray structure
Antibacterial activity

ABSTRACT

In the present study, a series of mononuclear Ni(II), Cu(II) and Zn(II) complexes with ONNO donor salen-type Schiff base ligands, derived from different 3,5-dihalosalicylaldehyde with polymethylenediamines of varying chain length, have been prepared. All the synthesized compounds were characterized by using various spectroscopic (FT-IR and ^{1}H NMR) and analytical (CHN etc.) techniques. Furthermore, three complexes (**ZnL^1, NiL^3** and **NiL^4**) were successfully characterized by single crystal X-ray diffraction. The data revealed that the geometry around Zn(II) was distorted square pyramidal for **ZnL^1**, while **NiL^3** and **NiL^4** complexes adapted slightly distorted octahedral geometries around Ni(II). The antibacterial activities of the synthesized ligands and their respective complexes were elaborated by screening them against two strains of Gram positive (*Staphylococcus aureus* and *Bacillus cereus*) and two strains of Gram negative (*Escherichia coli* and *Pseudomonas aeruginosa)* bacteria. It was found from the measurements of zones of inhibition that metal chelates are marginally more effective than free ligands.

1. Introduction

The species having imine bonds (–C=N–) are familiar with many names like imines, anils, Schiff bases and azomethines. These species can be prepared easily by the condensation of primary amine and aldehyde or ketones in a particular solvent [1]. These moieties are useful as chelating agents because of their structural diversity, easy mode of preparation and have a variety of applications in industry as well as in medicine [2–5].

A particular category of chelating Schiff base, salen, is synthesized when salicylaldehyde and diamine are condensed together in a 2:1 ratio. Salen-type ligands have the coordination number of four (ONNO), which can chelate with metal ion by making two covalent and two coordinate covalent bonds to adapt a *trans* planar geometry in addition to vacant axial position for ancillary ligand, analogous to porphyrins [6].

These salen-type ligands are considered among the most extensively studied ligands in coordination chemistry [7]. This is due to their adaptability, broad range of complexing behavior, catalytic, enzymatic, magnetic and pharmacological applications [8–11]. The beauty of salen type ligands is the facile reformation of the ligand's backbone and chelated transition metals ions which lead to the enhancement of antiproliferative, antioxidant and chemical properties of parent organic ligands [12–14]. Coordination of salen-type ligands with the metal atoms of 3d series specifically copper, nickel and zinc possess tunable electrical, spectroscopic, crystallographic, enzymatic and catalytic properties, and have rich structural functionality reliant on specific applications [15–20].

It was revealed from the literature survey that Ni complexes exhibit excellent antimicrobial, DNA binding activities, and also played a key role as catalyst in redox enzymes and hydrogenation reactions [21–22]. Copper complexes are active pharmacological species and are termed as potent inhibitors against cancer cells by stopping the uncontrolled extension of cell division. Copper complexes can crack the cell DNA *via* oxidative mechanism and hence can be considered as alternative to Cis-Platin [23–27]. Zinc,

* Corresponding author.
E-mail address: h.kargar@ardakan.ac.ir (H. Kargar).

https://doi.org/10.1016/j.molstruc.2021.130112
0022-2860/

a very effective bioactive metal, found in the human body and is a part of many enzymes like carbonic anhydrase, carboxypeptidase and alcohol dehydrogenase. A brief overview of literature is evident about the role of zinc complexes as antidepressant, anti-inflammatory and antimicrobial agents [28,29]

Keeping in mind about the large-scale applications and continuation of our previous work, here we planned to prepare new dihalogenated salen-type multidentate (ONNO) ligands and their complexes with Cu(II), Ni(II) and Zn(II) to elaborate their structural diversities and biological potential.

2. Experimental

2.1. Materials and physical measurements

The solvents, relevant precursors and other chemicals used in the present study were of analytical grade and purchased from Merck, Acros organics and Sigma Aldrich. Dynalon SMP10 equipped with a digital thermometer was used to measure the melting points of all the synthesized compounds. Microanalysis of the complexes were done using a Heraeus CHN–O-FLASH EA 1112 elemental analyzer. FT-IR spectra were recorded on a FT-IR Prestige 21 spectrophotometer from 4000–400 cm^{-1} using KBr pellets. ^1H NMR spectroscopy in DMSO–d_6 (400 MHz, Bruker) was carried out by using tetramethylsilane (TMS) as internal standard. Chemical shifts for proton resonances are reported in ppm (δ) relative to tetramethylsilane and DMSO–d_6.

2.2. General procedure for the synthesis of the Schiff bases (H_2L^x) ($x = 1$–4)

Same procedure was used for the synthesis of salen-type Schiff base ligands as reported earlier with some modifications [30]. 2 mmol of 3,5-dihalosalicylaldehyde was dissolved in 20 mL of ethanol in a round bottom flask (100 mL) to make a homogeneous solution. To this, 1 mmol of ethanolic solution (15 mL) of respective diamine was added and the reaction mixture was refluxed for 1–3 h by putting the flask over the water bath. On cooling to the room temperature the precipitates appeared which were filtered and washed thrice with absolute ethanol and finally dried in a desiccator containing anhydrous calcium chloride.

2.3. General procedure for the synthesis of the complexes

Acetates of Ni(II), Cu(II) and Zn(II) were used to prepare the aimed metal complexes (Scheme 1). Equimolar amounts of salen-type Schiff base ligands ($H_2\mathbf{L^x}$) were mixed with respective salt of metal acetates after complete dissolution in methanol and refluxed for 3 h till precipitation occurs. Each solid product was separated by filtration, washed by MeOH (30 mL) and after that kept under $CaCl_2$-dryness in a specific desiccators.

[Ni(L^1)], Calculated for $C_{16}H_{10}Br_4N_2NiO_2$: C 30.00, H 1.57, N 4.37%. Analysis found: C 31.13, H 1.51, N 4.46. FT-IR (KBr, cm^{-1}): υ C–H (aromatic): 3066, υ C–H (aliphatic): 2947, 2924, υ HC=N: 1620, υ C=C and C–N: 1581, 1506, 1442, 1373, υ C–O: 1321, υ Ni-N: 549, υ Ni-O: 410.

[Cu(L^1)], Calculated for $C_{16}H_{10}Br_4CuN_2O_2$: C 29.77, H 1.56, N 4.34%. Analysis found: C 29.64, H 1.49, N 4.21. FT-IR (KBr, cm^{-1}): υ C–H (aromatic): 3062, υ C–H (aliphatic): 2933, 2916, υ HC=N: 1628, υ C=C and C–N: 1577, 1504, 1433, 1377, υ C–O: 1301, υ Cu-N: 547, υ Cu-O: 420.

[Zn(L^1)], Calculated for $C_{16}H_{10}Br_4N_2O_2Zn$: C 29.69, H 1.56, N 4.33%. Analysis found: C 29.57, H 1.51, N 4.47. FT-IR (KBr, cm^{-1}): υ C–H (aromatic): 3066, υ C–H (aliphatic): 2931, 2899, υ HC=N: 1639, υ C=C and C–N: 1577, 1510, 1433, 1381, υ C–O: 1296, υ Zn-N: 547, υ Zn-O: 432. ^1H NMR [d_6-DMSO, δ (ppm)]: 8.45 (s, 2 H, **H**–C=N), 7.68 (d, 2 H, $J = 2.7$ Hz, **H** arom.), 7.44 (d, 2 H, $J = 2.7$ Hz, **H** arom.), 3.75 (s, 4 H, C**H**$_2$–N).

[Ni(L^2)], Calculated for $C_{16}H_{10}I_4N_2NiO_2$: C 23.19, H 1.22, N 3.38%. Analysis found: C 22.28, H 1.01, N 3.27. FT-IR (KBr, cm^{-1}): υ C–H (aromatic): 3047, υ C–H (aliphatic): 2918, 2850, υ HC=N: 1614, υ C=C and C–N: 1568, 1492, 1433, 1369, υ C–O: 1321, υ Ni-N: 545, υ Ni-O: 408.

[Cu(L^2)], Calculated for $C_{16}H_{10}CuI_4N_2O_2$: C 23.06, H 1.21, N 3.36%. Analysis found: C 23.19, H 1.17, N 3.23. FT-IR (KBr, cm^{-1}): υ C–H (aromatic): 3037, υ C–H (aliphatic): 2908, 2850, υ HC=N: 1616, υ C=C and C–N: 1564, 1487, 1427, 1371, υ C–O: 1296, υ Cu-N: 545, υ Cu-O: 415.

[Zn(L^2)], Calculated for $C_{16}H_{10}I_4N_2O_2Zn$: C 23.08, H 1.21, N 3.35%. Analysis found: C 22.98, H 1.27, N 3.42. FT-IR (KBr, cm^{-1}): υ C–H (aromatic): 3053, υ C–H (aliphatic): 2924, 2852, υ HC=N: 1635, υ C=C and C–N: 1564, 1506, 1425, 1402, υ C–O: 1305, υ Zn-N: 574, υ Zn-O: 424. ^1H NMR [d_6-DMSO, δ (ppm)]: 8.37 (s, 2 H, **H**–C=N), 7.93 (d, 2 H, $J = 2.4$ Hz, **H** arom.), 7.56 (d, 2 H, $J = 2.4$ Hz, **H** arom.), 3.73 (s, 4 H, C**H**$_2$–N).

[Ni(L^3)], Calculated for $C_{18}H_{14}Br_4N_2NiO_2$: C 32.33, H 2.11, N 4.19%. Analysis found: C 32.21, H 2.08, N 4.23. FT-IR (KBr, cm^{-1}): υ C–H (aromatic): 3070, υ C–H (aliphatic): 2922, 2852, υ HC=N: 1616, υ C=C and C–N: 1579, 1508, 1444, 1384, υ C–O: 1325, υ Ni-N: 532, υ Ni-O: 418.

[Cu(L^3)], Calculated for $C_{18}H_{14}Br_4CuN_2O_2$: C 32.10, H 2.10, N 4.16%. Analysis found: C 32.01, H 2.13, N 4.25. FT-IR (KBr, cm^{-1}): υ C–H (aromatic): 3068, υ C–H (aliphatic): 2920, 2850, υ HC=N: 1622, υ C=C and C–N: 1579, 1510, 1440, 1384, υ C–O: 1315, υ Cu-N: 549, υ Cu-O: 420.

[Zn(L^3)], Calculated for $C_{18}H_{14}Br_4N_2O_2Zn$: C 32.01, H 2.09, N 4.15%. Analysis found: C 32.14, H 2.05, N 4.03. FT-IR (KBr, cm^{-1}): υ C–H (aromatic): 3051, υ C–H (aliphatic): 2931, 2891, υ HC=N: 1620, υ C=C and C–N: 1574, 1502, 1444, 1409, υ C–O: 1315, υ Zn-N: 551, υ Zn-O: 420. ^1H NMR [d_6-DMSO, δ (ppm)]: 8.34 (s, 2 H, **H**–C=N), 7.67 (d, 2 H, $J = 2.6$ Hz, **H** arom.), 7.41 (d, 2 H, $J = 2.6$ Hz, **H** arom.), 3.36 (br, 4 H, C**H**$_2$–N), 1.85 (br, 4 H, C**H**$_2$–C).

[Ni(L^4)], Calculated for $C_{18}H_{14}I_4N_2NiO_2$: C 25.24, H 1.65, N 3.27%. Analysis found: C 25.13, H 1.67, N 3.18. FT-IR (KBr, cm^{-1}): υ C–H (aromatic): 3053, υ C–H (aliphatic): 2906, 2866, υ HC=N: 1612, υ C=C and C–N: 1566, 1500, 1435, 1406, υ C–O: 1319, υ Ni-N: 530, υ Ni-O: 410.

[Cu(L^4)], Calculated for $C_{18}H_{14}CuI_4N_2O_2$: C 25.10, H 1.64, N 3.25%. Analysis found: C 25.25, H 1.61, N 3.16. FT-IR (KBr, cm^{-1}): υ C–H (aromatic): 3051, υ C–H (aliphatic): 2922, 2850, υ HC=N: 1622, υ C=C and C–N: 1565, 1544, 1435, 1404, υ C–O: 1317, υ Cu-N: 545, υ Cu-O: 414.

[Zn(L^4)], Calculated for $C_{18}H_{14}I_4N_2O_2Zn$: C 25.04, H 1.63, N 3.24%. Analysis found: C 24.93, H 1.67, N 3.13. FT-IR (KBr, cm^{-1}): υ C–H (aromatic): 3035, υ C–H (aliphatic): 2931, 2868, υ HC=N: 1620, υ C=C and C–N: 1564, 1492, 1431, 1400, υ C–O: 1313, υ Zn-N: 555, υ Zn-O: 410. ^1H NMR [d_6-DMSO, δ (ppm)]: 8.27 (s, 2 H, **H**–C=N), 7.91 (d, 2 H, $J = 2.4$ Hz, **H** arom.), 7.53 (d, 2 H, $J = 2.4$ Hz, **H** arom.), 3.56 (br, 4 H, C**H**$_2$–N), 1.85 (br, 4 H, C**H**$_2$–C).

2.4. Crystallographic methods

For single crystal XRD inspection of **ZnL^1**, **NiL^3** and **NiL^4** complexes, Bruker Kappa APEXII CCD X-ray diffractometer was utilized possessing a graphite monochromated Mo-Kα radiation ($\lambda = 0.71073$ Å). Suitable single crystals were obtained from pyridine and DMF solution and fixed on a glass fiber for collecting reflections on Bruker Apex-II software [31]. In order to solve raw

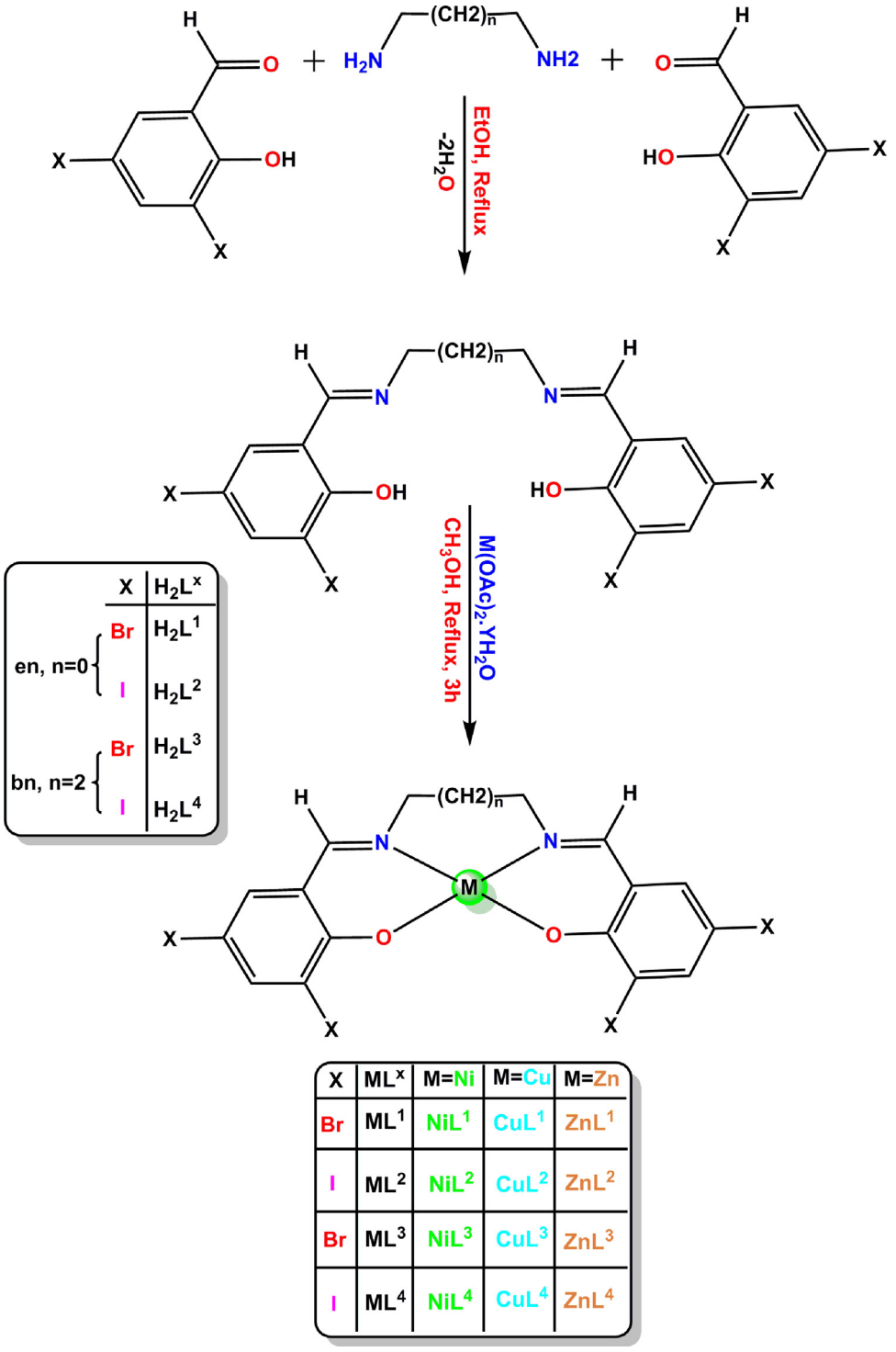

Scheme 1. Synthetic route of complexes.

data, SHELXS97 was employed [32] and then refined by utilizing anisotropic displacement parameters for all non-hydrogen atoms. International tables for X-ray Crystallography were utilized for atomic factors [33]. All the H-atoms were added to the structure from residual peaks and refined with relative isotropic displacement parameters. For refinement purposes, SHELXL-2018/3 and WinGX-2014.1 programs were utilized [34,35]. ω-scans method was employed for data collection and integrated using Bruker SAINT [36] software package. For pictorial view of **ZnL^1**, **NiL^3** and **NiL^4** ORTEP-3 [37] and platon were employed [38].

2.5. Biological activity evaluation

Evaluation of biological potential was carried out by *in vitro* screening of the synthesized compounds against the panel of two gram negative, *Escherichia coli* PTCC1394 and *Pseudomonas aeruginosa* PTCC1074 and two gram positive, *Staphylococcus aureus* PTCC1431 and *Bacillus cereus* PTCC1015 bacterial strains by adapting the disk diffusion method. This method is very convenient, efficient and has very low cost as compared to other procedures [39,40].

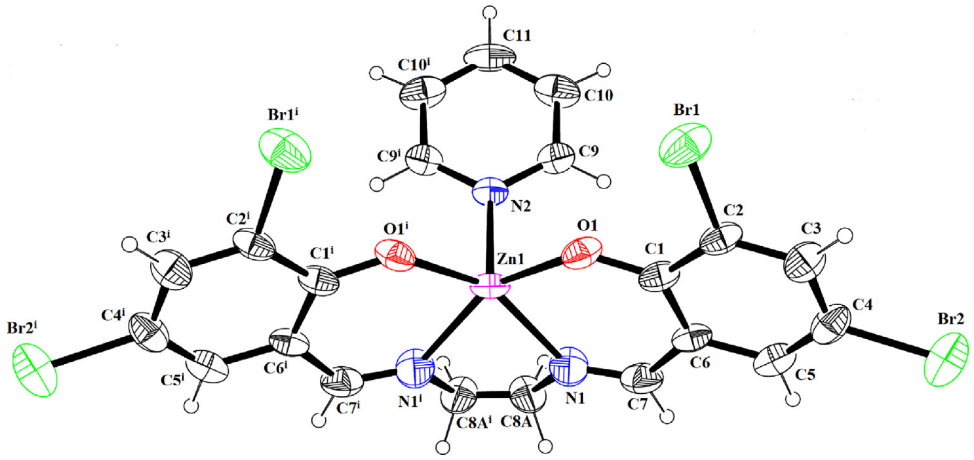

Fig. 1. ORTEP diagram of **ZnL[1]** drawn at the probability level of 30%. H-atoms are displayed by small circle of arbitrary radii.

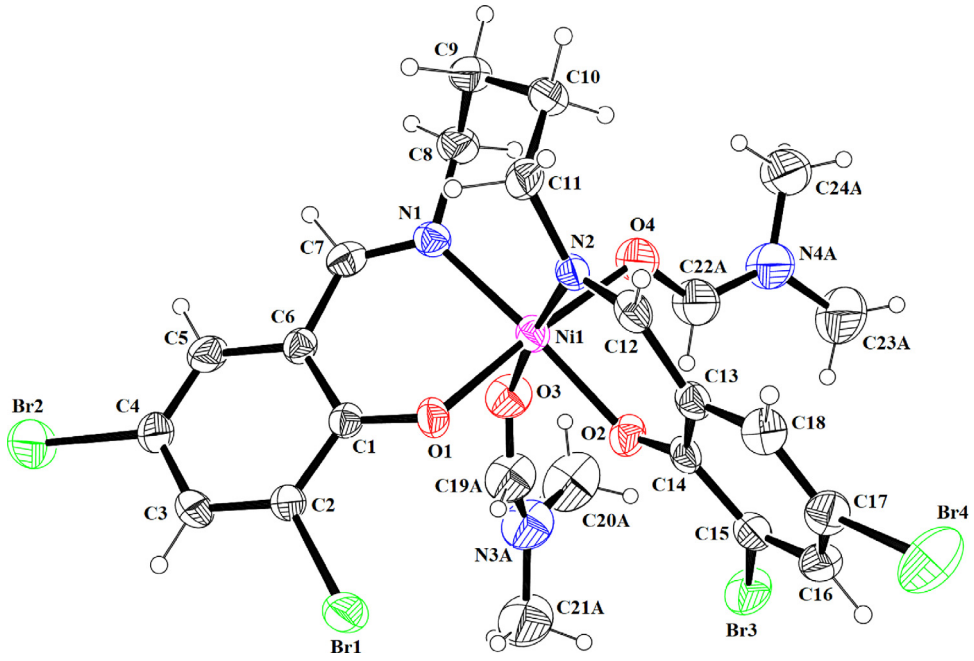

Fig. 2. ORTEP diagram of **NiL[3]** drawn at the probability level of 30%. H-atoms are displayed by small circle of arbitrary radii. Only major parts of disordered moieties are shown for clarity.

The most convenient solvent, dimethyl sulfoxide (DMSO), was used to prepare the stock solutions of the synthesized compounds because it has the ability to dissolve almost all kinds of transition metal complexes. Furthermore, it also acts a negative control and shows zero activity against the tested bacterial strains. The stock solutions were prepared by dissolving 20 mg of the sample in 20 mL of DMSO (1 mg/mL). Then the dilution method was applied to attain the concentration of 50 μg/mL for the preparation of laboratory samples. The population of bacterial strains was sub cultured by using an agar as nutrition media. Erythromycin and Ampicillin were chosen as standard antibacterial drugs to act as positive control for the sake of comparison under the provision of similar conditions.

Paper discs, with a diameter of 7 mm, made up of Whatman filter paper number 1 were sterilized before use in an autoclave. Then these sterilized paper discs were thoroughly saturated with the desired synthesized compounds or DMSO and placed aseptically in the petri dishes containing nutrient agar media inoculated with the above mentioned four bacteria separately and then incubated for 24 h at 37 °C. The diameters of zones of inhibitions created by the samples were measured in mm after an incubation period of 24 h.

3. Results and discussion

3.1. Syntheses

A series of four salen-type Schiff base ligands $H_2\mathbf{L^1}$–$H_2\mathbf{L^4}$ and their respective nickel(II), copper(II) and zinc(II) complexes were synthesized (Scheme 1). After synthesis various spectro analytical techniques were employed to elucidate the structural features of the synthesized compounds. It was found that all compounds were non-hygroscopic, stable at room temperature and have bright col-

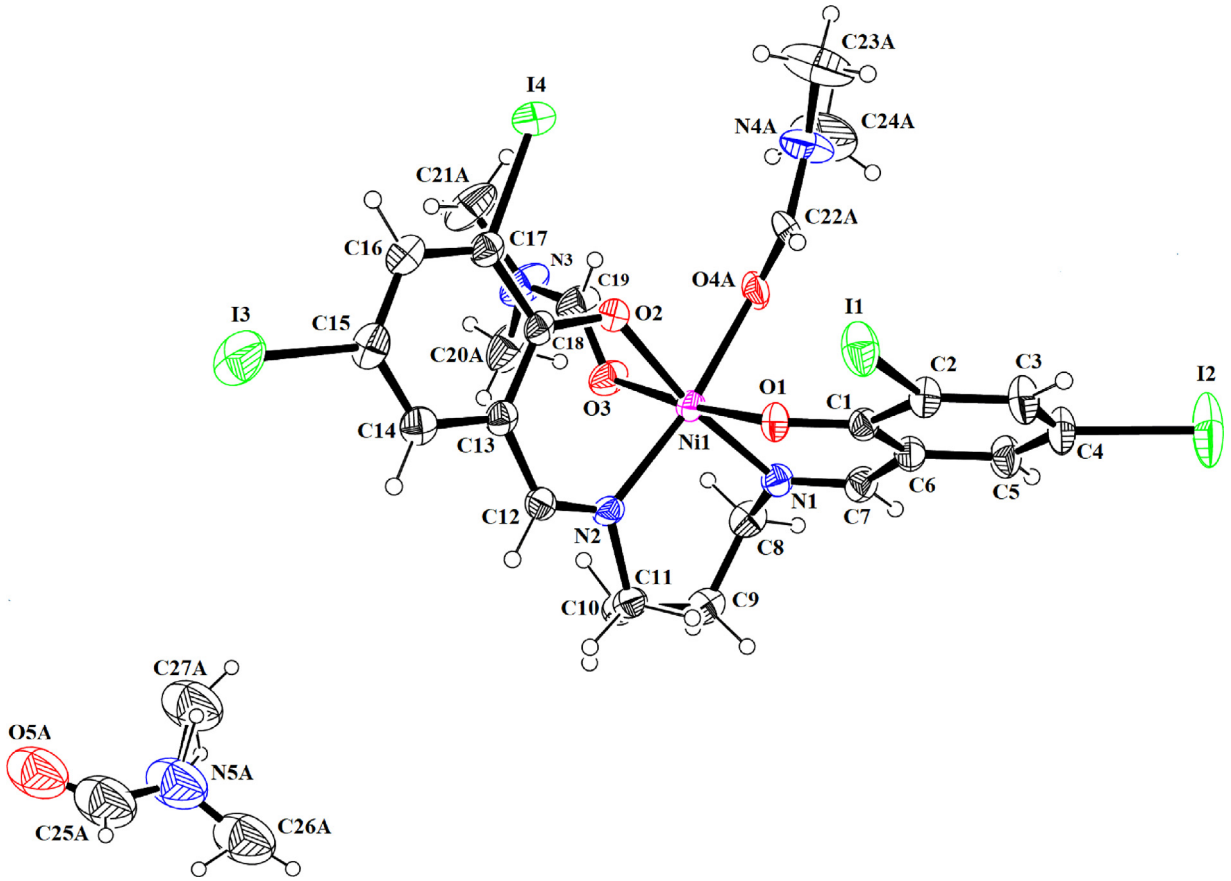

Fig. 3. ORTEP diagram of **NiL^4** drawn at the probability level of 30%. H-atoms are displayed by small circle of arbitrary radii. Only major parts of disordered moieties are displayed for clarity.

Table 1
Physical data of all complexes.

Compounds/molecular formula	Mol wt	Yield%	M. pt °C	Color
NiL^2/$C_{16}H_{10}I_4N_2NiO_2$	828.58	74	301	Red
NiL^3/$C_{18}H_{14}Br_4N_2NiO_2$	668.63	76	>400	Orange
NiL^4/$C_{18}H_{14}I_4N_2NiO_2$	856.63	74	261	Dark red
CuL^1/$C_{16}H_{10}Br_4CuN_2O_2$	645.43	77	295	Green
CuL^2/$C_{16}H_{10}CuI_4N_2O_2$	833.43	84	304	Dark green
CuL^3/$C_{18}H_{14}Br_4CuN_2O_2$	673.48	81	318	Brown
CuL^4/$C_{18}H_{14}CuI_4N_2O_2$	861.49	83	263	Orange
ZnL^1/$C_{16}H_{10}Br_4N_2O_2Zn$	647.26	76	351	Light yellow
ZnL^2/$C_{16}H_{10}I_4N_2O_2Zn$	835.27	75	291	Yellow
ZnL^3/$C_{18}H_{14}Br_4N_2O_2Zn$	675.32	65	341	Light yellow
ZnL^4/$C_{18}H_{14}I_4N_2O_2Zn$	863.32	68	257	Yellow

ors. A brief summary of some physical and analytical data is presented in Table 1.

The tetradentate (ONNO) chelating nature of the ligands (H_2**L$^{1-4}$**) was confirmed by FT-IR and ^{1}H NMR spectroscopic data.

3.2. Crystal structure descriptions of complexes

In **ZnL^1** (Fig. 1, Table 2), the central Zn-atom is coordinated by one chelating ligand (C1-C7/C8A/N1/O1/Br1/Br2), one symmetrically generated chelating ligand (C1^i-C7^i/C8A^i/N1^i/O1^i/Br1^i/Br2^i)) (i) (x, 1/2-y, z) and one non-chelating ligand (C9-C11/C9^i/C10^i/N2) containing two symmetry related C-atoms. Equatorial locations are occupied by two N-atoms and two O-atoms of the chelating ligand whereas apical location is occupied by N-atom (N2) of the pyridine ring. The bond lengths in coordination sphere range from 1.983 (4) to 2.086 (6) Å. Bond angles in equatorial plane range from 76.5 (3)° to 97.62 (2)° whereas the bond angles of apical atom (N2) with the atoms of the equatorial plane range from 101.05 (2)° to 103.2 (2)°. Zn-atom is deviated by 0.48 Å from the basal plane (N1/N1^i/O1/O1^i) indicating that the base of the geometry is not a perfect square. Thus, a distorted square pyramidal geometry is formed in **ZnL^1**. In (C1-C7/C8A/N1/O1/Br1/Br2), the (E)−3-iminoprop-1-en-1-ol group A (C1/C6/C7/N1/O1), 3,5-dibromobenznene ring B (C1-C6/Br1/Br2) and pyridine ring C (C9-C11/C9^i/C10^i/N2) are found to be planar with respective r.m.s deviation of 0.0100, 0.0252 and 0.0007 Å. The C-atom that is directly attached with the N-atom of moiety A is found to be disordered over two sets of sites with occupancy of each part is 1/2. The dihedral angles among A/B, A/C and B/C are 2.11 (2)°, 77.7 (2)° and 75.9 (2)°, respectively. The investigations of dihedral angles infer that group A and ring B are mainly parallel to each other. The molecules are interconnected through C–H···O and C–H···Br bonding to form one dimensional infinite chain along [100] crystallographic direction, where CH is from disordered C-atom which acts as donor (Fig. S1, Table 3). Besides H-bonding, a weak π-π stacking interaction is found which assists in further stabilization of crystal packing as displayed in Fig. S2.

In **NiL^3** (Fig. 2, Table 2), the central Ni-atom is coordinated by two N & two O-atoms from a chelating ligand, and two O-atoms from non-chelating ligands. In coordination sphere, Ni1-N1 and Ni1-O1 bond length ranges from 2.046 (4) to 2.038 (4) Å and 1.986 (4) to 2.155 (4) Å, respectively, whereas bond angles range from 83.18 (2)° to 96.44 (2)°. Bond angles and bond lengths are such that a slightly distorted octahedral geometry is formed. The (E)−3-iminoprop-1-en-1-ol group

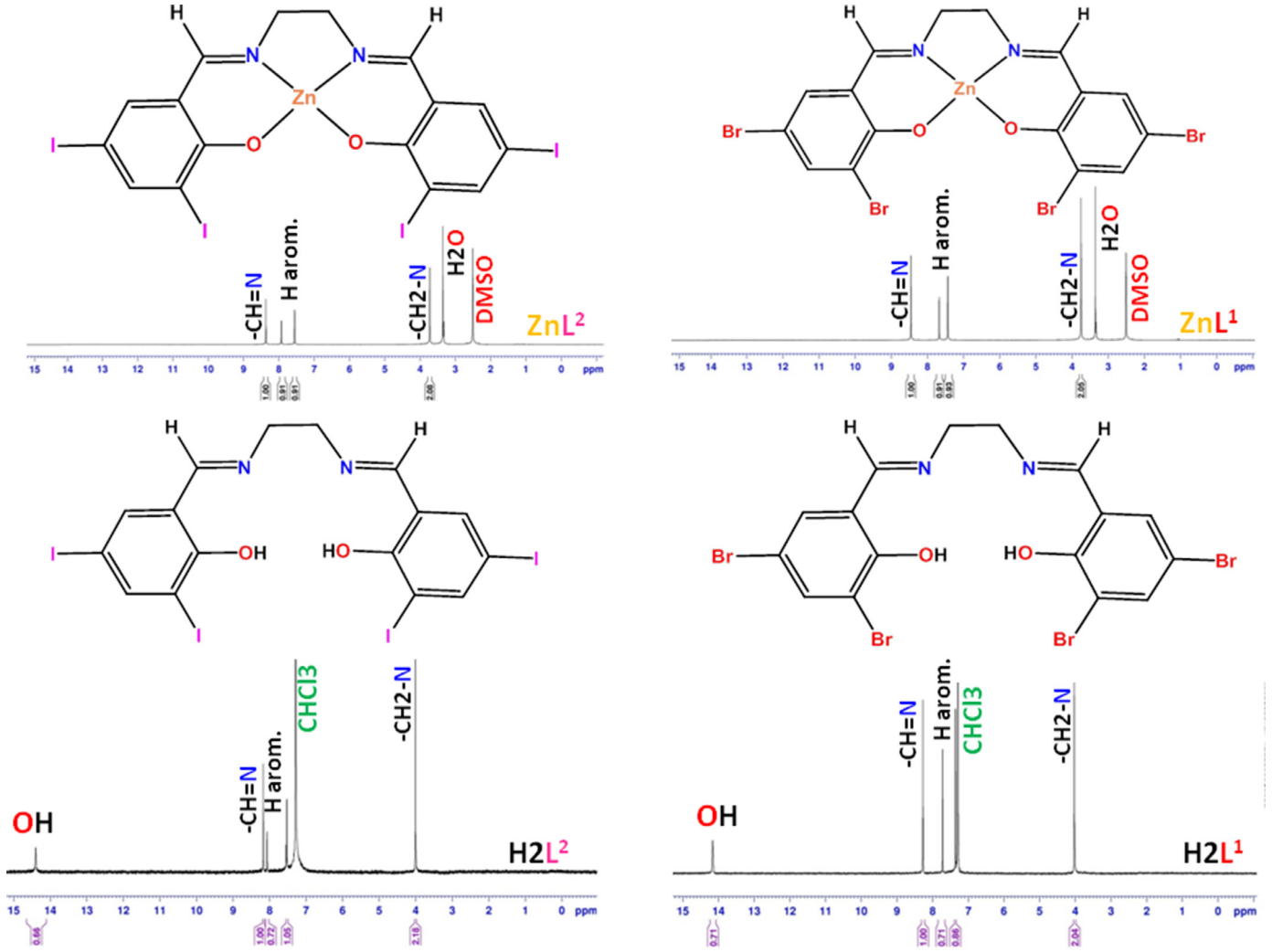

Fig. 4. ^{1}H NMR spectra of the H_2**L**^{1} and H_2**L**^{2} (Bottom) ligands in $CDCl_3$ and their **ZnL**^{1} and **ZnL**^{2} (Top) complexes in DMSO.

A (C1/C6/C7/N1/O1), 3,5-dibromobenznene ring B (C1-C6/Br1/Br2), basal plane C (C8/C10/C11/N1) of butane-1,4-diamine moiety (C8-C11/N1/N2), (E)−3-iminoprop-1-en-1-ol group D (C12-C14/N2/O2) and 3,5-dibromobenznene ring E (C13-C18/Br3/Br4) are found to be planar with respective r.m.s deviation of 0.0307, 0.0151, 0.0555, 0.0189 and 0.0208 Å. The apical (C9/N2) atoms are deviated by −0.6789 (7), 1.157 (6) Å, respectively below from the basal plane B. The dimethylformamide moiety of the first non-chelating ligand (C19-C21/N3/O3) is disordered with occupancy ratio of 0.608 (1): 0.392(1). The major part F (C19A-C21A/N3A) and the minor part G (C19B-C21B/N3B) are found to be planar with respective r.m.s deviation of 0.0512 and 0.0312 Å, the dihedral angle of 23.7 (4)° is found between F and G moieties. The dimethylformamide moiety of the second non-chelating ligand (C22-C24/N4/O4) is also disordered with occupancy ratio of 0.608 (1): 0.392(1). The major part H (C22A-C24A/N4A) and the minor part I (C22B-C24B/N4B) are found to be planar with respective r.m.s deviation of 0.0025 and 0.0583 Å, the dihedral angle of 41.2 (2)° is found among H and I moieties. Ring Puckering Analysis shows that the first chelating ring (C1/C6/C7/N1/Ni1) adapts nearly half chair conformation with puckering amplitude Q = 0.314(3) Å, θ = 59.7(7)° and φ = 14.4 (10)° whereas the second chelating ring (C12-C14/N2/O2/Ni1) adapts nearly S-form with puckering amplitude Q = 0.090(4) Å, θ = 63(3)° and φ = 329(3)°. The dihedral angles among A/B, A/C, C/D and D/E are 1.6 (2)°, 48.7 (2)°, 57.4 (2)° and 4.4 (2)°, respectively. The investigation of dihedral angles shows that group A and ring B are mainly parallel to each other. Various weak intramolecular H-bonding of type C–H···O are found that assist in the stable configuration of the crystal structure. Various S (5) loops are found with the distance between donor hydrogen and acceptor oxygen ranges from 2.35 to 2.52 Å as displayed in Fig. S3 and specified in Table 3. The molecules are interconnected by weak C–H···π interaction to form infinite chains along [010] direction as displayed in Fig. S4.

In **NiL**^{4} (Fig. 3, Table 2), the central Ni-atom is coordinated by two N and two O-atoms from a chelating ligand and two O-atoms from non-chelating ligands. In coordination sphere, Ni1-N1 and Ni1-O1 bond length ranges from 2.038 (4) to 2.050 (4) Å and 1.985 (4) to 2.271 (3) Å, respectively whereas bond angles range from 83.13 (2)° to 97.27 (2)°. Bond angles and bond lengths are such that a slightly distorted octahedral geometry is formed. The (E)−3-iminoprop-1-en-1-ol group A (C1/C6/C7/N1/O1), 3,5-diiodobenznene ring B (C1-C6/I1/I2), basal plane C (C8/C11/C12/N1) of butane-1,4-diamine moiety (C8-C11/N1/N2), (E)−3-iminoprop-1-en-1-ol group D (C12/C13/C18/N2/O2) and 3,5-diiodobenznene ring E (C13-C18/I3/I4) are found to be planar with respective r.m.s deviation of 0.0347, 0.0155, 0.0866, 0.0302 and 0.0342 Å. The apical (C11) atom is deviated by 0.4709 (9) Å from the basal plane B. In the first non-chelating ligand (C19/C20A/C21A/N3/O3), the terminal C-atoms are disordered with occupancy ratio 0.56(3):

Table 2
Crystal data and structure refinement parameters for **ZnL[1], NiL[3]** and **NiL[4]** complexes.

Identification code	ZnL^1	NiL^3	NiL^4
Chemical formula	$C_{21}H_{15}Br_4N_3O_2Zn$	$C_{24}H_{28}Br_4N_4NiO_4$	$C_{26.25}H_{33.25}I_4N_{4.75}NiO_{4.75}$
Formula weight	726.37	814.85	1057.63
Temperature (K)	296	296	296
Radiation type	Mo *Kα*	Mo *Kα*	Mo *Kα*
Wavelength (Å)	0.71073	0.71073	0.71073
Crystal system	Orthorhombic	Triclinic	Triclinic
Space group	*Pnma*	$P\bar{1}$	$P\bar{1}$
a (Å)	7.3940(9)	9.5133(5)	9.6767(5)
b (Å)	23.504(4)	12.5026(7)	12.7208(8)
c (Å)	13.083(2)	15.2114(9)	16.1316(10)
α (°)	90	110.469(3)	68.776(2)
β (°)	90	93.407(3)	89.955(2)
γ (°)	90	103.105(3)	76.598(2)
Volume ($Å^3$)	2273.8(6)	1631.69(16)	1793.05(19)
Z	4	2	2
Calculated Density (Mg/m^3)	2.122	1.659	1.959
Absorption coefficient (mm^{-1})	8.134	5.525	4.022
F(000)	1392	800	1004
Crystal Shape	Needle	Needle	Prism
Crystal color	Light yellow	Green blue	Light yellow
Crystal size (mm)	0.28 × 0.16 × 0.16	0.42 × 0.22 × 0.20	0.30 × 0.25 × 0.20
Data Collection			
Diffractometer	Bruker KAPPA APEXII CCD Diffractometer	Bruker KAPPA APEXII CCD Diffractometer	Bruker KAPPA APEXII CCD diffractometer
Absorption correction	multi-scan (SADABS; Bruker, 2007)	multi-scan (SADABS; Bruker, 2007)	multi-scan (SADABS; Bruker, 2007)
No. of measured, independent and observed [$I > 2s(I)$] reflections	19,052, 2547, 1193	24,576, 7089, 4099	27,356, 7823, 5890
R_{int}	0.089	0.038	0.030
Theta range for data collection	3.031° to 27.000°	2.224° to 27.142°	1.773° to 27.107°
Index ranges	$-9 \le h \le 9$, $-30 \le k \le 30$, $-16 \le l \le 16$	$-11 \le h \le 12$, $-16 \le k \le 15$, $-20 \le l \le 20$	$-12 \le h \le 12$, $-16 \le k \le 16$, $-20 \le l \le 20$
$(\sin\theta/\lambda)_{max}$ ($Å^{-1}$)	0.639	0.642	0.641
Refinement			
$R[F^2 > 2\sigma(F^2)]$, $wR(F^2)$, *S*	0.046, 0.106, 1.00	0.048, 0.131, 1.02	0.045, 0.122, 1.04
No. of reflections	2547	7089	7823
No. of parameters	155	415	424
No. of restraints	10	234	175
H-atom treatment	H-atom parameters constrained	H-atom parameters constrained	H-atom parameters constrained
$\Delta\rho_{max}$, $\Delta\rho_{min}$ (e $Å^{-3}$)	0.51, −0.68	1.03, −0.97	1.62, −1.84

0.44(3). All the atoms of the second non-chelating ligand are disordered with occupancy ratio 0.56(3): 0.44(3). The dihedral angles among A/B, A/C, C/D and D/E are 1.76 (3)°, 62.95 (2)°, 17.3 (3)° and 6.33 (2)°, respectively. The investigation of dihedral angle shows that group A and ring B are almost parallel to each other; similarly, moiety D and ring E are also almost parallel to each other. In the asymmetric unit, 75% solvent molecule of dimethylformamide is there which is also disordered over two set of locations with occupancy ratio of 0.417(3): 0.333(3) refined by making anisotropic displacement parameters of all the disordered atoms equal. Various weak intramolecular H-bonding of type C–H···O are found that assist in the stable configuration of the crystal structure. Various S (5) loops are found with the distances between donor hydrogen and acceptor oxygen ranges from 2.41 to 2.66 Å as displayed in Fig. S5 and specified in Table 3. The Bis(dimethylformamide)-(*N,N'*-bis(3,5-diiodosalicylidene)−1,4-diaminobutane)-nickel(II) molecules are jointed with solvent molecules through weak C–H···O bonding as displayed in Fig. S6 and specified in Table 2. Furthermore, Bis(dimethylformamide)-(*N,N'*-bis(3,5-diiodosalicylidene)−1,4-diaminobutane)-nickel(II) molecules are jointed among themselves through weak C–H···N and C–H···I bonding as given in Table 3. Another weak interaction of type C–H···π is found which assists in further strengthening of crystal packing as displayed in Fig. S7.

3.3. ^1H NMR spectra

The ^{1}H NMR spectra of the synthesized salen type Schiff bases were taken in deuterated chloroform, while deuterated dimethyl sulfoxide (DMSO–d_6) was used to record the spectra of zinc complexes (**ZnL[1]-ZnL[4]**). The details of chemical shift values of the tested compounds are presented in experimental section. One of the important chemical shift (δ) values in the form of singlets present at 14.15, 14.39, 14.74 and 14.92 ppm in the ^{1}H NMR spectra of the ligands H_2**L[1]**, H_2**L[2]**, H_2**L[3]** and H_2**L[4]** respectively, confirm the presence of aromatic OH. These values appeared very down field in the recorded spectra due to the involvement of phenolic protons in hydrogen bonding. These phenolic peaks vanished on the coordination of ligands with the zinc metals as evident from Figs. 4 and 5.

Another key evidence of complexation of ligands with metals is the slight down field shifts of signals of azomethine protons at 8.45, 8.37, 8.34 and 8.27 ppm for **ZnL[1], ZnL[2], ZnL[3]** and **ZnL[4]** complexes, respectively. Hence, phenolic oxygen and azomethine nitrogen are the binding sites available for coordination with zinc metal. The protons of aromatic rings of Zn(II) complexes appeared in the range of 7.41–7.93 ppm in the form of doublets. The –CH_2–N protons of the **ZnL[1]** and **ZnL[2]** complexes appeared as a singlet at δ = 3.75 and 3.73 ppm, respectively. The broad signals at δ = 3.36,

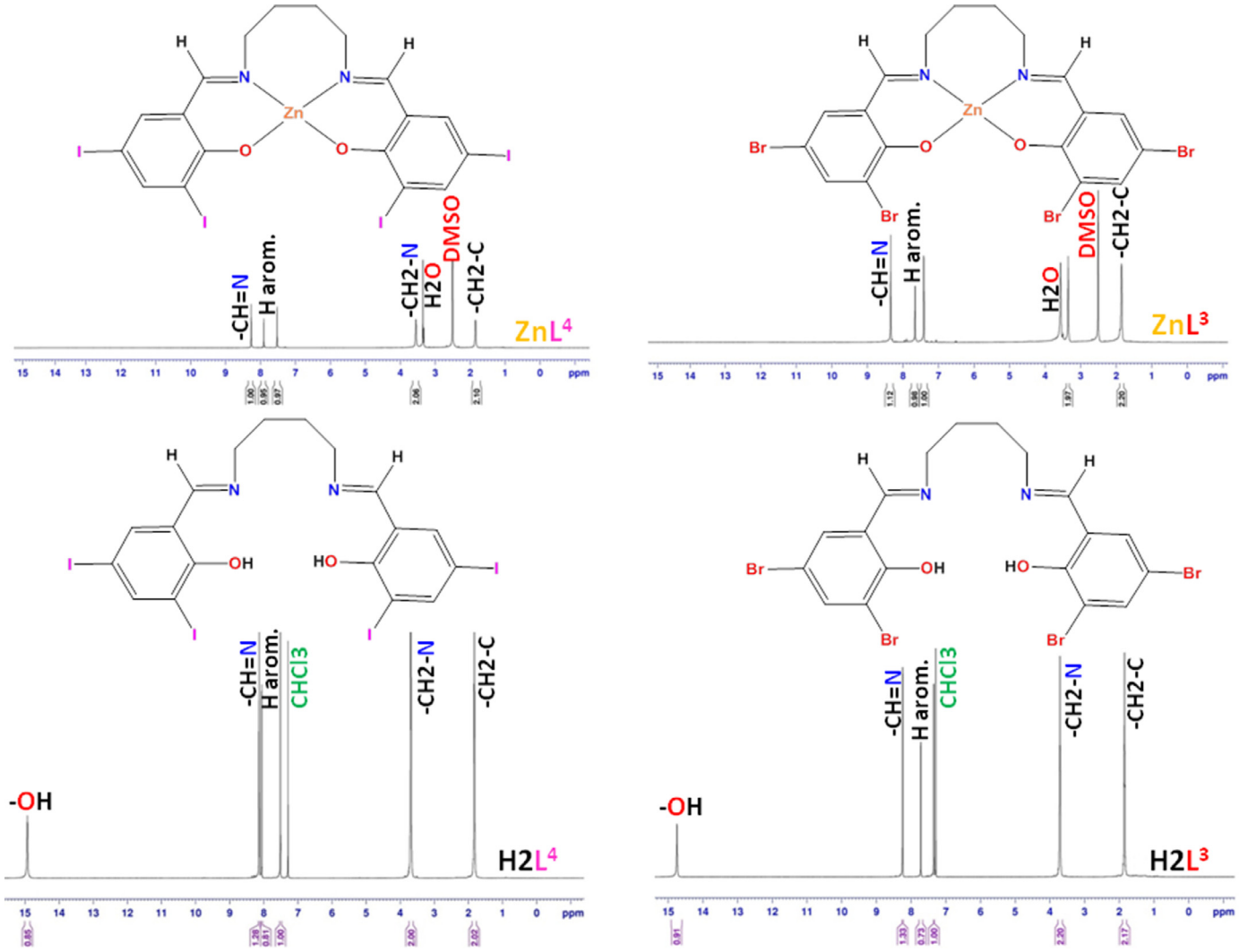

Fig. 5. ^{1}H NMR spectra of the H_2**L**^{3} and H_2**L**^{4} (Bottom) ligands in $CDCl_3$ and their **ZnL**^{3} and **ZnL**^{4} (Top) complexes in DMSO.

3.56 and 1.85 ppm are assigned to the $-CH_2-N$ and $-CH_2-C$ protons of the **ZnL**^{3} and **ZnL**^{4} complexes, respectively.

3.4. FT-IR spectra

The comparison between the selected bands in the FT-IR spectra of Schiff base ligands and their metal complexes are presented in experimental part and shown in Figs. 6 and 7. In the FT-IR spectra of complexes, the ν (-CH=N) and ν (C–O) bands shifted to lower and higher wavenumbers, respectively, in comparison with their corresponding free ligands thereby indicating a coordinative interaction between the iminic nitrogen and phenolic oxygen atoms with central metals. This coordination could also be confirmed by the appearance of weak bands located at the lower wavenumbers which are assigned to (M–N) and (M–O) at about 530 to 574 cm^{-1} and 409 to 432 cm^{-1} respectively.

3.5. Antibacterial activity

The antibacterial action of the synthesized compounds and standard drugs was checked by screening against four species of bacterial strains and the data is summarized in Table 4 and in Fig. 8 in the form of histogram. A careful observation of the results indicated that tested compounds were active against the screened microbial species. The tested compounds bear comparable activities against parent standard drugs, Erythromycin and Ampicillin. The results suggested, a little bit, enhanced antibacterial activity of complexes in comparison with the free ligands. This amplification in the activities against bacterial pathogens can be assumed on the basis of Overtone's concept and Tweedy's chelation theory [41]. The decrease in the number of active bacterial cells on the treatment with these compounds may be attributed on the basis of cell permeability and lipophilicity. The ligands were found to be active probably due to the presence of hydroxyl function and azomethine chromophore which may lead to the formation of hydrogen bonding with active centers of the cells constituting the cell membrane and hence the permeability was increased [42]. A slight increase in the activity of the ligands on chelation might be due to change in the polarity of cation on account of hybridization of filled orbitals of ligands with empty "d" orbitals of the metals [43,44]. The increased lipophilicity can be addressed owing to the delocalization of π electrons on chelation which covers the whole chelate ring which leads to the facilitated perforation through lipid bilayer membrane to destroy the pathogens [45]. Another concept is that these metal complexes can also affect the process of respiration of

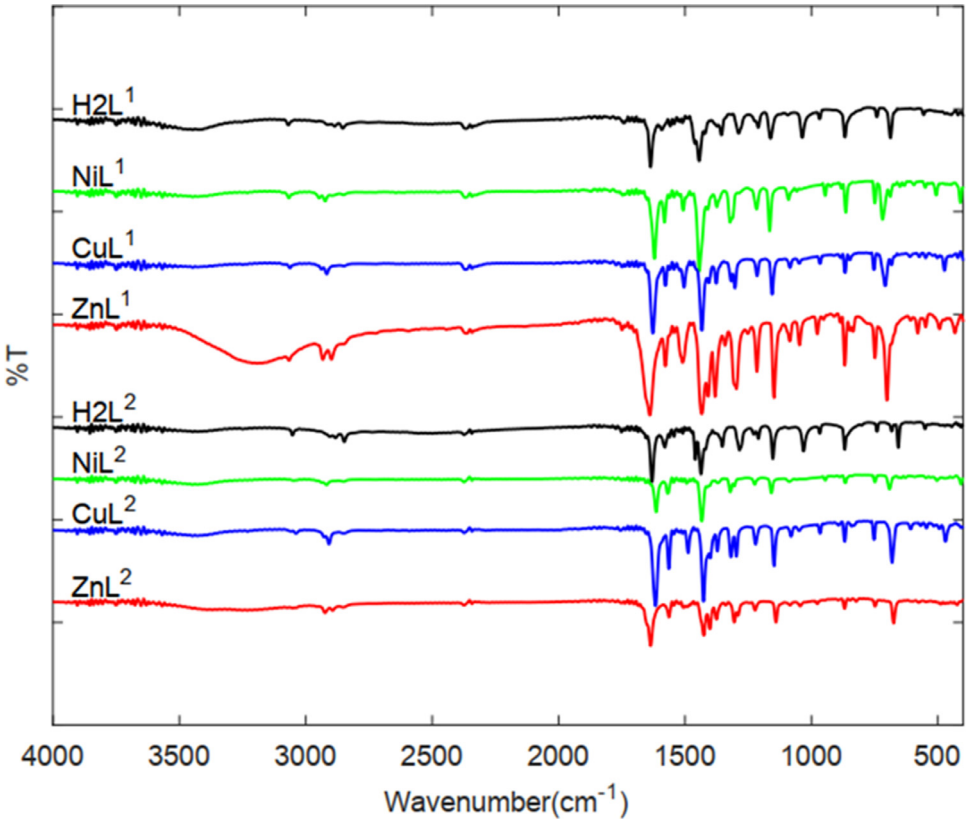

Fig. 6. FT-IR spectra of the H_2**L**^{1} and H_2**L**^{2} ligands and their corresponding complexes.

Table 3
Hydrogen-bond geometry (Å, °) for **ZnL**^{1}, **NiL**^{3} and **NiL**^{4} complexes.

ZnL^1	*D*—H···*A*	*D*—H	H···*A*	*D*···*A*	*D*—H···*A*
	C8*A*—H8*A1*···Br1^{i}	0.97	2.63	3.432 (17)	140
	C8*B*—H8*B2*···O1^{ii}	0.97	2.56	3.505 (16)	166
	C9—H9···Br2^{iii}	0.93	2.98	3.633 (7)	129
	C10—H10···Br1^{iv}	0.93	3.08	3.738 (7)	129
NiL^3	***D*—H···*A***	***D*—H**	**H···*A***	***D*···*A***	***D*—H···*A***
	C19*A*—H19*A*···O1	0.93	2.52	3.07(2)	119
	C20*A*—H20*C*···O3	0.96	2.39	2.780 (12)	104
	C8—H8*B*···O4	0.97	2.46	3.112 (7)	124
	C22*A*—H22*A*···O2	0.93	2.44	2.87 (2)	108
	C24*A*—H24*A*···O4	0.96	2.35	2.764 (12)	105
	C*—*H*···*π	***C*—H**	**H···*π***	***C*···*π***	***C*—H···*π***
		0.96	2.77	3.603(18)	54
		0.96	2.91	3.373 (15)	39
		0.96	2.96	3.373 (15)	31
NiL^4	***D*—H···*A***	***D*—H**	**H···*A***	***D*···*A***	***D*—H···*A***
	C7—H7···O5*B*^{vii}	0.93	2.58	3.43 (3)	139
	C8—H8*B*···O3	0.97	2.47	3.123 (7)	125
	C19—H19···O2	0.93	2.41	2.886 (7)	112
	C20*A*—H20*B*···I4^{i}	0.96	3.18	3.94 (2)	137
	C20*B*—H20*E*···I4^{i}	0.96	3.33	4.28 (4)	170
	C20*B*—H20*F*···N3^{viii}	0.96	2.68	3.52 (5)	147
	C22*A*—H22*A*···O1	0.93	2.66	3.14 (2)	113
	C22*B*—H22*B*···O2	0.93	1.98	2.63 (3)	126
	C23*B*—H23*D*···O5*B*^{viii}	0.96	2.65	3.40 (4)	135
	C25*A*—H25*A*···I2^{ix}	0.93	3.08	3.91 (4)	150
	C26*A*—H26*B*···I2^{ix}	0.96	3.22	4.00 (3)	139
	C25*B*—H25*B*···I1^{x}	0.93	3.18	3.98 (4)	146
	C27*B*—H27*F*···I5*A*	0.96	2.00	2.56 (5)	115
	C*—*H*···*π	***C*—H**	**H···*π***	***C*···*π***	***C*—H···*π***
	C24*A*—H24*A*···Cg1^{vi}	0.96	2.84	3.76(3)	159
	C20*A*—H20*A*···Cg2^{vi}	0.96	2.55	3.42(3)	150

Symmetry codes: (i) $x + 1, y, z$; (ii) $x + 1/2, y, -z + 3/2$; (iii) $-x + 1, -y + 1, -z + 1$; (iv) $x + 1/2, y, -z + 1/2$: (v) –x,1-y,2-z; (vi) –x,-y,1-z; (vii) $x, y - 1, z + 1$; (viii) $-x, -y + 1, -z + 1$; (ix) $-x + 1, -y, -z + 1$; (x) $x + 1, y + 1, z - 1$.

Table 4
Antibacterial activity of Schiff base ligands and its complexes.

Diameter of zone of inhibition (mm) Compound	*E. coli*	*P. aeruginosa*	*S. aureus*	*B. cereus*
H_2L^1	12	12	22	19
NiL^1	14	13	24	22
CuL^1	13	14	23	21
ZnL^1	14	14	24	23
H_2L^2	12	12	26	22
NiL^2	14	13	27	24
CuL^2	14	13	27	25
ZnL^2	13	15	29	26
H_2L^3	15	13	21	23
NiL^3	17	15	22	25
CuL^3	16	14	23	26
ZnL^3	16	15	24	25
H_2L^4	11	12	25	22
NiL^4	13	13	26	24
CuL^4	13	13	27	24
ZnL^4	12	13	27	25
Control (DMSO)	–	–	–	–
Standard (Erythromycin)	16	17	25	24
Standard (Ampicillin)	11	14	27	26

cells, leading to the blockage in the synthesis of proteins causing the death of organisms [46,47].

It is worth noting from the zones of inhibition, created by tested compounds, that ligands and their respective metal complexes are moderately more potent inhibitors of gram positive rather than gram negative bacterial strains. This is because gram positive bacteria have thick peptidoglycan layer without outer lipid membrane while gram negative bacteria have thin peptidoglycan layer and have an outer lipid membrane [48].

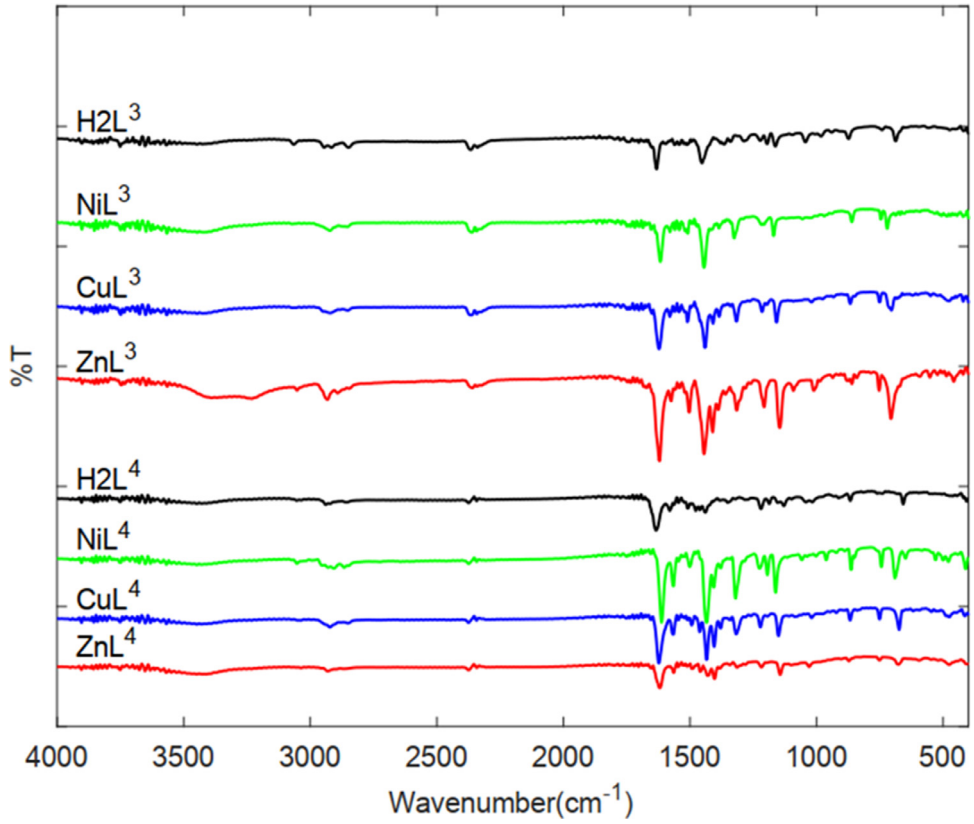

Fig. 7. FT-IR spectra of the H_2**L**^{3} and H_2**L**^{4} ligands and their corresponding complexes.

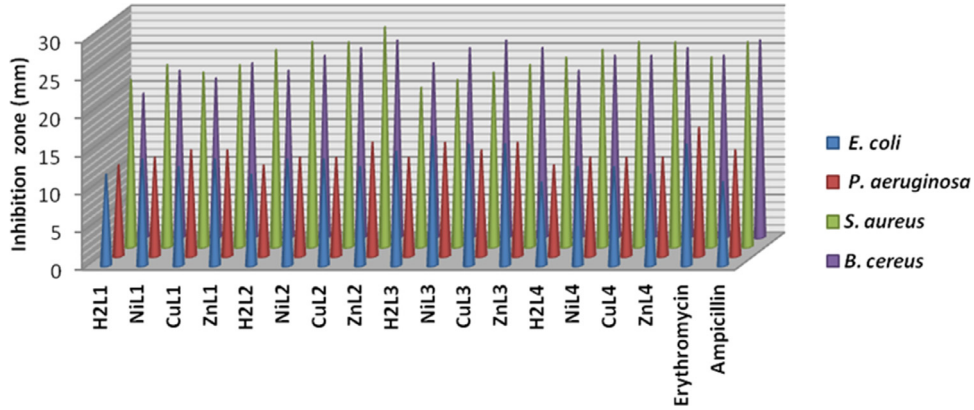

Fig. 8. A histogram show the antibacterial evaluation of the investigated Schiff base ligands and its complexes.

4. Conclusion

In the current research work, we have synthesized and characterized some new mononuclear metal complexes containing ONNO donor salen-type Schiff base ligands. The synthesized complexes were characterized by using various physicochemical methods. Furthermore, the molecular structures of certain complexes have been confirmed by single crystal X-ray diffraction. The results showed that the ligand to metal stoichiometry in complexes is 1:1. A distorted square pyramidal geometry for **ZnL**^{1} and slightly distorted octahedral geometries for **NiL**^{3} and **NiL**^{4} were proposed for Schiff base metal complexes. The *in vitro* biological screening experiments inferred that the compounds showed satisfactory inhibitory effects against most of the tested microbes and metal complexes were found to be faintly more active than the free Schiff base ligands. Also, the inhibition zones of the Schiff base ligands and corresponding metal complexes showed that the all compounds were more toxic towards gram positive strains than gram negative strains.

Appendix A. Supplementary data

CCDC No. 2036048 (for **ZnL**^{1}), CCDC No. 2036049 (for **NiL**^{3}) and CCDC No. 2039058 (for **NiL**^{4}) contain the supplementary crystallographic data for this contribution. Copies of the data may be obtained free of charges on application to CCDC, 12 Union Road, Cambridge CB2 1 EB, UK (Fax: +44–1223–336–033; E-mail: deposit@ccdc.cam.ac.uk or http://www.ccdc.cam.ac.uk).

Authors' statement

We would like to make a statement about the author's main contribution: HK and AAA synthesized all the compounds, and characterized them by different techniques; AAA was responsible

for biological data acquisition and analysis; MNT, MA and KSM collected the single-crystal X-ray diffraction data and determined the structures. HK wrote the manuscript with input from all authors. All authors discussed the results and commented on the manuscript.

Declaration of Competing Interest

The authors declare that they have no conflict of interest.

Acknowledgment

The support of this work by Ardakan University is gratefully acknowledged.

Supplementary materials

Supplementary material associated with this article can be found, in the online version, at doi:10.1016/j.molstruc.2021.130112.

References

[1] H. Alamgholiloo, S. Zhang, A. Ahadi, S. Rostamnia, R. Banaei, Z. Li, X. Liu, M. Shokouhimehr, Synthesis of bimetallic 4-PySI-Pd@Cu(BDC) via open metal site Cu-MOF: effect of metal and support of Pd@Cu-MOFs in H_2 generation from formic acid, Mol. Catal. 467 (2019) 30–37.
[2] H. Alamgholiloo, S. Rostamnia, A. Hassankhani, J. Khalafy, M.M. Baradarani, G. Mahmoudi, X. Liu, Stepwise post-modification immobilization of palladium Schiff-base complex on to the OMS-Cu (BDC) metal–organic framework for Mizoroki-Heck cross-coupling reaction, Appl. Organomet. Chem. 32 (2018) e4539.
[3] H. Kargar, V. Torabi, A. Akbari, R. Behjatmanesh-Ardakani, A. Sahraei, M.N. Tahir, Synthesis, crystal structure, spectroscopic investigations and computational studies of Ni(II) and Pd(II) complexes with asymmetric tetradentate NOON Schiff base ligand, Struct. Chem. 30 (2019) 2289–2299.
[4] H. Kargar, V. Torabi, A. Akbari, R. Behjatmanesh-Ardakani, A. Sahraei, M.N. Tahir, Pd(II) and Ni(II) complexes containing an asymmetric Schiff base ligand: synthesis, x-ray crystal structure, spectroscopic investigations and computational studies, J. Mol. Struct. 1205 (2020) 127642.
[5] H. Kargar, R. Behjatmanesh-Ardakani, V. Torabi, A. Sarvian, Z. Kazemi, Z. Chavoshpour-Natanzi, V. Mirkhani, A. Sahraei, M.N. Tahir, M. Ashfaq, Novel copper(II) and zinc(II) complexes of halogenated bidentate N,O-donor Schiff base ligands: synthesis, characterization, crystal structures, DNA binding, molecular docking, DFT and TD-DFT computational studies, Inorg. Chim. Acta 514 (2021) 120004.
[6] M.A. Malik, O.A. Dar, P. Gull, M.Y. Wani, A.A. Hashmi, Heterocyclic Schiff base transition metal complexes in antimicrobial and anticancer chemotherapy, Med. Chem. Comm. 9 (2018) 409–436.
[7] D.A. Atwood, M.J. Harvey, Group 13 compounds incorporating salen ligands, Chem. Rev. 101 (2001) 37–52.
[8] Z. Zhou, W. Li, X. Hou, L. Chen, X. Hao, C. Redshaw, W.H. Sun, Synthesis, structure and photophysical properties of 2-benzhydryl-4-methyl-6-(aryliminomethyl)phenol ligands and the zinc complexes thereof, Inorg. Chim. Acta 392 (2012) 292–299.
[9] S. Bhunora, J. Mugo, A. Bhaw-Luximon, S. Mapolie, J. Van Wyk, J. Darkwa, E. Nordlander, The use of Cu and Zn salicylaldimine complexes as catalyst precursors in ring opening polymerization of lactides: ligand effects on polymer characteristics, Appl. Organomet. Chem. 25 (2011) 133–145.
[10] X. Qiao, Z.Y. Ma, C.Z. Xie, F. Xue, Y.W. Zhang, J.Y. Xu, Z.Y. Qiang, J.S. Lou, G.J. Chen, S.P. Yan, Study on potential antitumor mechanism of a novel Schiff base copper(II) complex: synthesis, crystal structure, DNA binding, cytotoxicity and apoptosis induction activity, J. Inorg. Biochem. 105 (2011) 728–737.
[11] B.S. Creaven, B. Duff, D.A. Egan, K. Kavanagh, G. Rosair, V.R. Thangella, M. Walsh, Anticancer and antifungal activity of copper(II) complexes of quinolin-2(1H)-one-derived Schiff bases, Inorg. Chim. Acta 363 (2010) 4048–4058.
[12] D.C. Culita, L. Dyakova, G. Marinescu, T. Zhivkova, R. Spasov, L. Patron, R. Alexandrova, O. Oprea, Synthesis, characterization and cytotoxic activity of co(ii), ni(ii), cu(ii), and zn(ii) complexes with nonsteroidal antiinflamatory drug isoxicam as ligand, J. Inorg. Organomet. Polym. Mater. 29 (2019) 580–591.
[13] J. Cheng, K. Wei, X. Ma, X. Zhou, H. Xiang, Synthesis and photophysical properties of colorful salen-type Schiff bases, J. Phys. Chem. C117 (2013) 16552–16563.
[14] A. Haikarainen, J. Sipilä, P. Pietikäinen, A. Pajunen, I. Mutikainen, Synthesis and characterization of bulky salen-type complexes of Co, Cu, Fe, Mn and Ni with amphiphilic solubility properties, J. Chem. Soc. (2001) 991–995 Dalton Trans..
[15] S.C. Bhatia, J.M. Bindlish, A.R. Saini, P.C. Jain, Crystal and molecular structure of bis(N-allylsalicylideneiminato)-nickel(II) and -copper(II), J. Chem. Soc., Dalton Trans. (1981) 1773–1779.
[16] J.M. Bindlish, S.C. Bhatia, P.C. Jain, Preparation and crystallographic data of allylsalicyladiminato complexes of Ni(II), Pd(II) and Co(II), Indian J. Chem. 13 (1975) 81–82.
[17] R.P. Kashyap, J.M. Bindlish, P.C. Jain, Crystallographic data of bis(N-allylsalicylaldiminato) copper (II) monohydrate, Indian J. Chem. 11 (1973) 388–389.
[18] J.M. Bindlish, S.C. Bhatia, P. Gautam, P.C. Jain, Crystal and molecular structure of bis(N-allylsalicylaldiminato)-palladium(II), Indian J. Chem., Sect. A16 (1978) 279–282.
[19] H. Kargar, R. Kia, A.A. Ardakani, M.N. Tahir, Bis(dimethylformamide-κO){4,4′,6,6′-tetrachloro-2,2-[butane-1,4-diyl(nitrilomethanylylidene)] diphenolatoκ^4O,N,N′,O′}nickel(II), Acta Crystallogr. E68 (2012) m997.
[20] H. Kargar, R. Kia, A.A. Ardakani, M.N. Tahir, {4,4′,6,6′-Tetraiodo-2,2′-[propane-1,3-diylbis(nitrilomethanylylidene)]-diphenolato-κ^4O,N,N′,O′}nickel(II), Acta Crystallogr. E68 (2012) m1090.
[21] H. Kargar, A.A. Ardakani, M.N. Tahir, M. Ashfaq, K.S. Munawar, Synthesis, spectral characterization, crystal structure determination and antimicrobial activity of Ni(II), Cu(II) and Zn(II) complexes with the Schiff base ligand derived from 3,5-dibromosalicylaldehyde, J. Mol. Struct. 1229 (2021) 129842.
[22] R.N. Patel, S.P. Rawat, M. Choudhary, V.P. Sondhiya, D.K. Patel, K.K. Shukla, D.K. Patel, Y. Singh, R. Pandey, Synthesis, structure and biological activities of mixed ligand copper(II) and nickel(II) complexes of N′-(*1E*)-[(5-bromo-2-hydroxyphenyl)methylidene]benzoylhydrazone, Inorg, Chimica Acta 392 (2012) 283–291.
[23] H. Kargar, R. Behjatmanesh-Ardakani, V. Torabi, M. Kashani, Z. Chavoshpour–Natanzi, Z. Kazemi, V. Mirkhani, A. Sahraei, M.N. Tahir, M. Ashfaq, K.S. Munawar, Synthesis, characterization, crystal structures, DFT, TD-DFT, molecular docking and DNA binding studies of novel copper (II) and zinc (II) complexes bearing halogenated bidentate N,O-donor Schiff base ligands, Polyhedron 195 (2021) 114988.
[24] S. Tabassum, S. Amir, F. Arjmand, C. Pettinari, F. Marchetti, N. Masciocchi, G. Lupidi, R. Pettinari, Mixed-ligand Cu(II)evanillin, Schiffbase complexes; effect of coligands on their DNA binding, DNA cleavage, SOD mimetic and anticancer activity, Eur. J. Med. Chem. 60 (2013) 216–232.
[25] C. Marzano, M. Pellei, F. Tisato, C. Santini, Copper complexes as anticancer agents, Antican. Age. Med. Chem. 9 (2009) 185–211.
[26] H. Kargar, F. Aghaei-Meybodi, R. Behjatmanesh-Ardakani, M.R. Elahifard, V. Torabi, M. Fallah-Mehrjardi, M.N. Tahir, M. Ashfaq, K.S. Munawar, Synthesis, crystal structure, theoretical calculation, spectroscopic and antibacterial activity studies of copper(II) complexes bearing bidentate Schiff base ligands derived from 4-aminoantipyrine: influence of substitutions on antibacterial activity, J. Mol. Struct. 1230 (2021) 129908.
[27] S.O. Bahaffi, A.A.A. Aziz, M.M. El-Naggar, Synthesis, spectral characterization, DNA binding ability and antibacterial screening of copper(II) complexes of symmetrical NOON tetradentate Schiff bases bearing different bridges, J. Mol. Struct. 1020 (2012) 188–196.
[28] A. Rauf, A. Shah, K.S. Munawar, S. Ali, M.N. Tahir, M. Javed, A.M. Khan, Synthesis, physicochemical elucidation, biological screening and molecular docking studies of a Schiff base and its metal(II) complexes, Arab, J. Chem. 13 (2020) 1130–1141.
[29] G. Ramesh, S. Daravath, M. Swathi, V. Sumalatha, D.S. Shankar, Investigation on Co (II), Ni (II), Cu (II) and Zn (II) complexes derived from quadridentate salen-type Schiff base: structural characterization, DNA interactions, antioxidant proficiency and biological evaluation, Chem. Data Coll. 28 (2020) 100434.
[30] A.A. Ardakani, H. Kargar, N. Feizi, M.N. Tahir, Synthesis, characterization, crystal structures and antibacterial activities of some Schiff bases with N_2O_2 donor sets, J. Iran. Chem. Soc. 15 (2018) 1495–1504.
[31] APEX2, Bruker AXS Inc., Madison, Wisconsin, USA, (2013).
[32] G.M. Sheldrick, A short history of SHELX, Acta Crystallogr. A64 (2008) 112–122.
[33] W. Parrish, J. Langford, International Tables for Crystallography, in: A.J.C. Wilson (Ed.), Kluwer, Dordrecht, (1992) 48–50.
[34] G.M. Sheldrick, Crystal structure re finement with SHELXL, Acta Crystallogr. C71 (2015) 3–8.
[35] L.J. Farrugia, WinGX and ORTEP for windows: an update, J. Appl. Crystallogr. 45 (2012) 849–854.
[36] SAINT, Bruker AXS Inc., Madison, Wisconsin, USA, (2013).
[37] M.N. Burnett, C.K. Johnson, ORTEP-III Report ORNL-6895 Oak Ridge National Laboratory, Tennessee, USA (1996)
[38] A.L. Spek, Structure validation in chemical crystallography, Acta Crystallogr. D65 (2009) 148–155.
[39] K.H. Kailas, J.P. Sheetal, P.P. Anita, H.P. Apoorva, Four synthesis methods of Schiff base ligands and preparation of their metal complex with IR and antimicrobial investigation, World J. Pharm. Pharm. Sci. 5 (2016) 1055–1063.
[40] P.R. Murray, E.J. Baron, M.A. Pfaller, F.C. Tenover, R.H. Yolke, Manual of Clinical Microbiology, ASM, Washington, DC, USA, 1995.
[41] B.G. Tweedy, Plant extracts with metal ions as potential antimicrobial agents, Phytopatology 55 (1964) 910–918.
[42] A. Marir, T.N. Mouas, B. Anak, E. Jeanneau, A. Djedouani, L. Aribi-Zouioueche, F. Rabilloud, Cobalt (II), Nickel (II) and Zinc (II) complexes based on DHA: synthesis, X-ray crystal structure, antibacterial activity and DFT computational studies, J. Mol. Struct. 1217 (2020) 128353.
[43] K. Kralova, K. Kissova, O. Svajlenova, J. Vanco, Biological activity of copper(ii)-salicylideneaminoacidato complexes. Reduction of chlorophyll content in freshwater alga chloralla vulgaris and inhibition of photosynthetic electron transport in spinach chloroplasts, Chem. Pap. 58 (2004) 357–361.
[44] J. Parekh, P. Inamdhar, R. Nair, S. Baluja, S. Chanda, Synthesis and antibacterial activity of some Schiff bases derived from 4-aminobenzoic acid, J. Serb. Chem. Soc. 70 (2005) 1155–1161.

[45] A. Sahraei, H. Kargar, M. Hakimi, M.N. Tahir, Synthesis, characterization, crystal structures and biological activities of eight-coordinate zirconium(IV) Schiff base complexes, Transition Met. Chem. 42 (2017) 483–489.
[46] A. Sahraei, H. Kargar, M. Hakimi, M.N. Tahir, Distorted square-antiprism geometry of new zirconium (IV) Schiff base complexes: synthesis, spectral characterization, crystal structure and investigation of biological properties, J. Mol. Struct. 1149 (2017) 576–584.
[47] R. Nair. A. Shah, S. Baluja, S. Chanda, Synthesis and antibacterial activity of some Schiff base complexes, J. Serb. Chem. Soc. 71 (2006) 733–744.
[48] G. Kumar, D. Kumar, S. Devi, R. Johari, C.P. Singh, Synthesis, spectral characterization and antimicrobial evaluation of Schiff base Cu (II), Ni (II) and Co (II) complexes, Eur. J. Med. Chem. 45 (2010) 3056–3062.